

Article

## Conductivity-Dependent Flow Field-Flow Fractionation of Fulvic and Humic Acid Aggregates

Martha J. M. Wells

EnviroChem Services, 224 Windsor Drive, Cookeville, TN 38506, USA;

E-Mail: info@envirochemservices.net or mjmwells@tntech.edu; Tel.: +1-931-979-6808

Academic Editor: Ronald Beckett

Received: 22 July 2015 / Accepted: 15 September 2015 / Published: 22 September 2015

---

**Abstract:** Fulvic (FAs) and humic acids (HAs) are chemically fascinating. In water, they have a strong propensity to aggregate, but this research reveals that tendency is regulated by ionic strength. In the environment, conductivity extremes occur naturally—freshwater to seawater—warranting consideration at low and high values. The flow field flow fractionation (flow FFF) of FAs and HAs is observed to be concentration dependent in low ionic strength solutions whereas the corresponding flow FFF fractograms in high ionic strength solutions are concentration independent. Dynamic light scattering (DLS) also reveals insight into the conductivity-dependent behavior of humic substances (HSs). Four particle size ranges for FAs and humic acid aggregates are examined: (1) <10 nm; (2) 10 nm–6 μm; (3) 6–100 μm; and (4) >100 μm. Representative components of the different size ranges are observed to dynamically coexist in solution. The character of the various aggregates observed—such as random-extended-coiled macromolecules, hydrogels, supramolecular, and micellar—as influenced by electrolytic conductivity, is discussed. The disaggregation/aggregation of HSs is proposed to be a dynamic equilibrium process for which the rate of aggregate formation is controlled by the electrolytic conductivity of the solution.

**Keywords:** water quality; dissolved organic carbon (DOC); electrolytic conductivity; ionic strength; dynamic light scattering (DLS); macromolecular; supramolecular

---

## 1. Introduction

Natural organic matter (NOM) is to the environmental sciences what proteins, nucleic acids, lipids, and carbohydrates are to the life sciences. All of these materials possess unique properties determined by their size, folding, and patterns at the nanoscale. The study of NOM is a very old, yet currently provocative, topic. Humic substances (HSs) comprise a major fraction of NOM, and reportedly represent up to 60%–70% of total organic carbon (TOC) in soils and 60%–90% of dissolved organic carbon (DOC) in natural water [1]. Soil scientists have studied the chemical nature of HSs for two centuries, and their composition and conformation have been intensely researched. However, because of their complex nature, the primary, secondary, tertiary, and quaternary molecular arrangements of the fulvic (FAs) and humic (HAs) comprising TOC/DOC still remains ill defined.

This research is based on the hypothesis that multiple types of disaggregated/aggregated/coiled/extended/micelles/pseudomicelles/micelle-like/vesicles/supramolecular/fractal/nanogel/microgel conformations of HSs exist, depending on concentration and solution physicochemistry, such as pH, ionic strength, and the nature of counterions in solution. Ultimately, increased understanding of the relationship between NOM composition, conformation, aggregation, and chemical reactivity will benefit society by improving potable water production and wastewater treatment of emerging contaminants.

This manuscript attempts to address a scientific conundrum: *Why is the flow field-flow fractionation (FFF) of FAs and HAs concentration independent at high ionic strength and concentration dependent at low ionic strength?* The aim of this paper is to knit together seemingly disparate puzzle pieces from experiments in flow FFF and dynamic light scattering (DLS) to postulate an answer to this quandary.

The answer to this question hinges upon our fundamental understanding of the aggregation of HSs in solution, and conversely, our understanding of the aggregation of HSs in solution informs the answer to this question. The purpose of this manuscript is to focus on HS aggregation and not to get into the terminology fray of whether to call the aggregates extended/coiled/micelles/pseudomicelles/micelle-like/vesicles/supramolecular/fractal/nanogel/or microgel entities. In fact, variable types of these entities may coexist [2]. The data presented here indicate the presence and size of aggregates and is not designed to absolutely define their character. Therefore, the terminology “aggregates” and “aggregation phenomena” will be preferred with two exceptions: (1) the terminology used by researchers in a cited reference will be restated and used without judgment; and (2) the term “micelle” will be retained in describing the physical measurement referred to as the “critical micelle concentration”.

## 2. Experimental Section

This manuscript provides enhanced data analysis of previously published investigations; therefore, detailed experimental procedures exist in each of the publications cited [3,4]. Briefly, the channel dimensions of the apparatus used for symmetrical flow FFF were 28.5 cm (tip-to-tip length) × 2 cm (breadth) × 0.0508 cm (width). The membrane consisted of polypropylene-backed polysulfone having a molecular weight cutoff of 10,000.

The low conductivity mobile phase was composed of HPLC-grade water containing a surfactant, FL-70, 0.05% (Fisher Scientific, Fair Lawn, NJ, USA) and sodium azide, 0.03% (pH 7) (Fisher Scientific). The channel flow was 0.6 mL·min<sup>-1</sup>, while the cross flow was 3.1 mL·min<sup>-1</sup>. The stop flow was initiated

after 15 s and terminated after 2 min. The high conductivity mobile phase consisted of 0.095 M dibasic potassium phosphate, 0.005 M monobasic potassium phosphate, and 0.03% sodium azide in HPLC grade water (pH 8.1). Flow FFF was conducted with a cross flow rate of  $0.4 \text{ mL} \cdot \text{min}^{-1}$ , a channel flow rate of  $0.2 \text{ mL} \cdot \text{min}^{-1}$ , and a stop flow period of 7.5 min. The stop flow was initiated after 2.5 min and terminated after 10 min.

The hydrodynamic diameter of particles was calculated for normal mode flow FFF using Equation (1):

$$R \approx \frac{2 k T V^0}{\pi \eta V_c w^2 d} \quad (1)$$

where  $R$  is the retention ratio equal to the void time of the channel divided by the emergence time of the species,  $V_c$  is the channel volumetric flow rate and  $V$  is the void volume,  $w$  is the channel width,  $k$  is the Boltzmann's constant,  $T$  is the absolute temperature,  $d$  is the hydrodynamic diameter of the diffusing particle, and  $\eta$  is the solution viscosity. The hydrodynamic diameter is calculated for particles eluting in steric (lift) mode flow FFF using Equation (2):

$$R \approx \frac{3 d}{w} \quad (2)$$

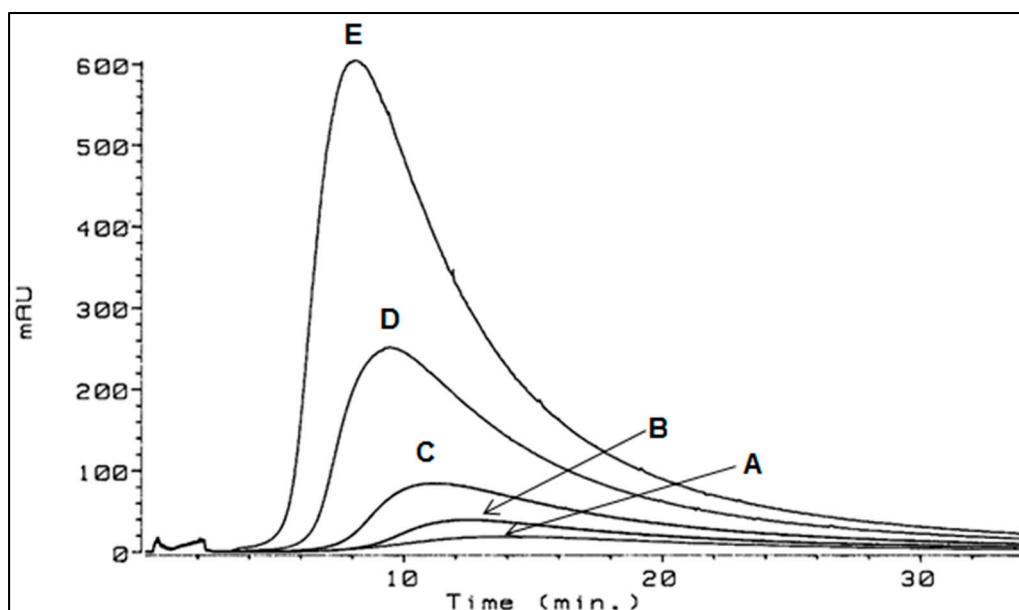
The diffusion coefficient ( $D$ ) is related to the hydrodynamic diameter by the Stokes-Einstein equation:

$$D = \frac{k T}{3 \pi \eta d} \quad (3)$$

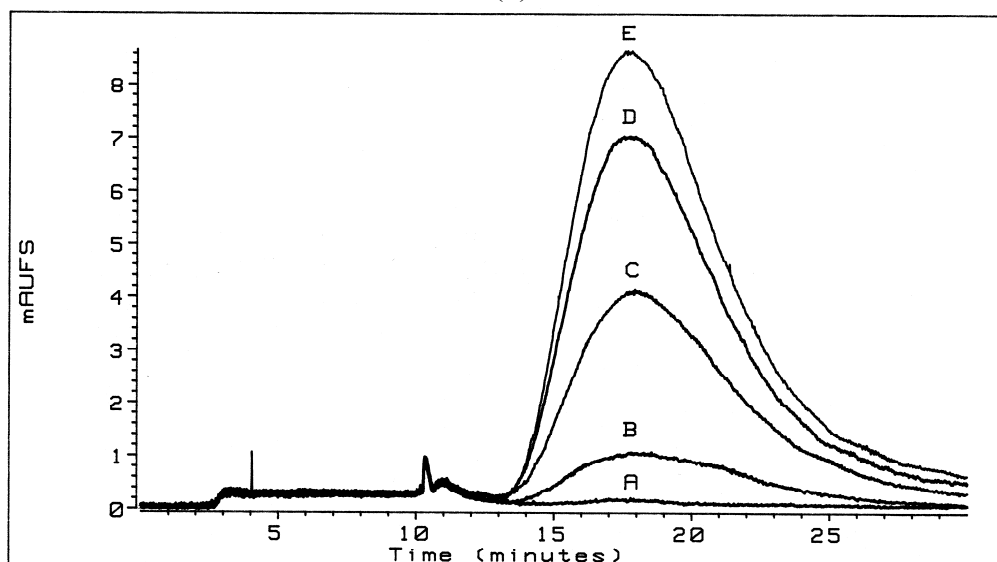
assuming the aggregate is spherical.

### 3. Results and Discussion

Concentration independence in an analytical procedure is a requirement for quantitative measurement. Consequently, concentration dependence is anathema to analytical chemists. Previously, the concentration dependence of HSs in flow FFF at low ionic strength [5,6] and the concentration independence at high ionic strength [4] was observed (Figure 1). Lead *et al.* [7] also demonstrated the trend toward a less broad and more Gaussian distribution of the flow FFF fractograms of Suwannee River FA as the ionic strength of the mobile phase increased. To investigate the conductivity-dependent behavior of HSs and postulate an answer to the question—*Why is the flow field-flow fractionation of fulvic and humic acids concentration independent at high ionic strength and concentration dependent at low ionic strength?*—various, seemingly unrelated, experiments in flow FFF and DLS at low and high ionic strength will be examined and compared.



(a)



(b)

**Figure 1.** (a) Flow field flow fractionation (flow FFF) fractograms of Aldrich HA in low electrolytic conductivity solutions (0.05% surfactant/0.03%  $\text{NaN}_3$ ) for A—1.1, B—2.6, C—5.2, D—10.3, and E—20.0 mg/mL detected by  $\text{UV}_{254}$  [5]; (b) flow FFF fractograms of Aldrich HA in high electrolytic conductivity solutions (0.095 M dibasic potassium phosphate, 0.005 M monobasic potassium phosphate, and 0.03 percent  $\text{NaN}_3$ ) following removal by activated carbon (A represents 64 mg of activated carbon added, B—32 mg, C—16 mg, D—4 mg, and E—0 mg) added to the initial concentration (E) of 5.1 mg/L detected by  $\text{UV}_{270}$  [4]. Figure 1b reproduced by permission of The Royal Society of Chemistry.

### 3.1. Flow Field-Flow Fractionation (Flow FFF) of Humic Substances (HSs)

In these experiments, the flow FFF membrane consisted of polypropylene-backed polysulfone having a molecular weight cutoff of 10,000 Da. However, FAs and HAs ranging in weight-average molecular weight from 750 to 3400 were retained in the system [3,4]. Monitoring the cross-flow revealed no detectable loss of analytes through the membrane. The negatively charged polysulfone membrane is postulated to repel the negatively charged polyelectrolytic humic macromolecules causing them to be retained in the channel.

#### 3.1.1. Low Electrolytic Conductivity Solutions

In low ionic strength solution, the retention times of Aldrich HA (Aldrich Corporation, Milwaukee, WI, USA) and polystyrene sulfonate (PSS,  $M_w = 5400$ ) (Polysciences, Inc., Warrington, PA, USA) decreased as concentration increased (Figure 2). Additionally, at concentrations of approximately 5 mg/mL and greater, the retention order of the HA and the PSS is reversed relative to that observed at approximately 1 mg/mL. Rather than concluding that these data result from a shift to lower values of the measured particle size as concentration increases [6], it is alternatively here proposed that as concentration increased above 5 mg/mL, particle size increased.

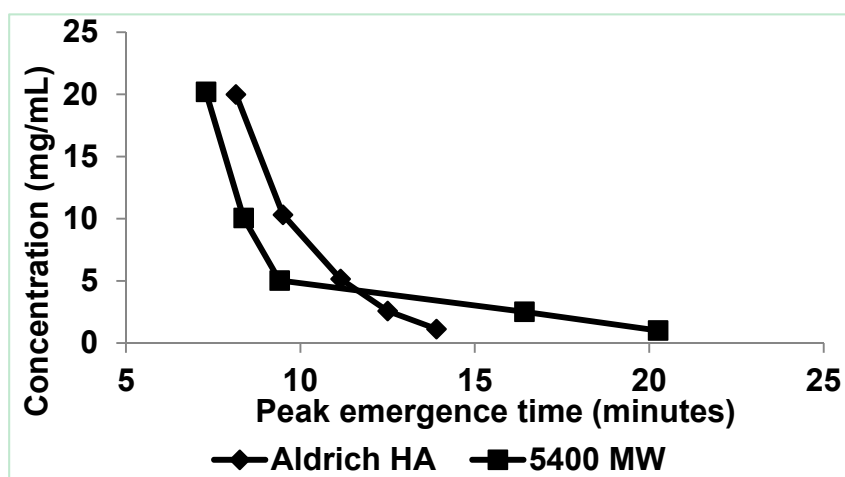


**Figure 2.** Flow FFF emergence time dependence on concentration for polystyrene sulfonate ( $M_w = 5400$  Da) at 20.2, 10.1, 5.0, 2.5, and 1.0 mg/mL and Aldrich HA at 20.0, 10.3, 5.2, 2.6, and 1.1 mg/mL in low electrolytic conductivity solution (0.05% surfactant/0.03%  $\text{NaN}_3$ ) [5].

This behavior is postulated to result from increased aggregation, *i.e.*, increased size, of the humic acid aggregate as concentration increased, resulting in a change in the separation mechanism from predominantly normal (Brownian) mode flow FFF to predominantly steric (hyperlayer or lift) mode flow FFF (Figure 3). The steric inversion point in flow FFF has been reported to occur at approximately 1  $\mu\text{m}$  [8]; it is also influenced by shape.

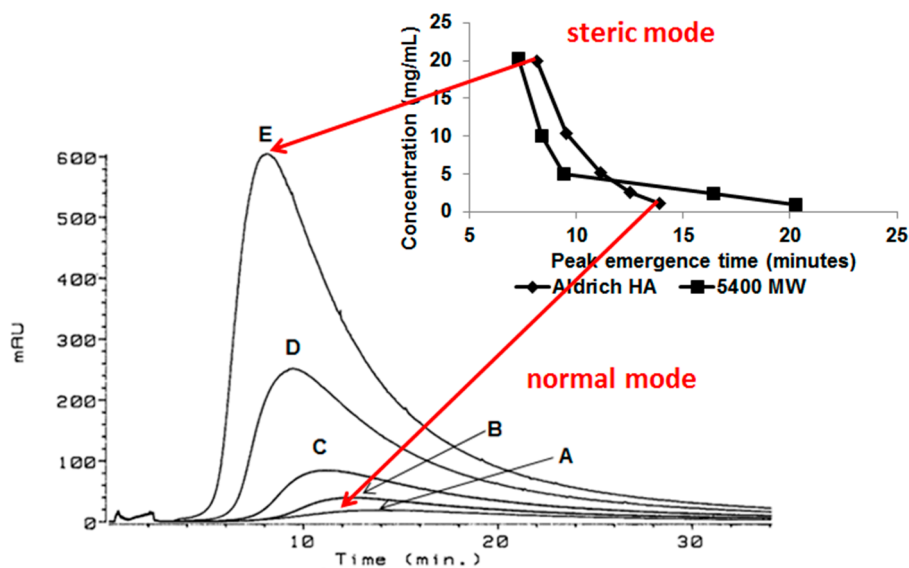


**Figure 3.** Separation mechanism conversion from predominantly normal (Brownian) mode flow FFF to predominantly steric (hyperlayer or lift) mode flow FFF. Flow FFF fractograms of Aldrich HA in low electrolytic conductivity solutions (0.05% surfactant/0.03%  $\text{NaN}_3$ ) for A—1.1, B—2.6, C—5.2, D—10.3, and E—20.0 mg/mL detected by  $\text{UV}_{254}$ ; inset: flow FFF emergence time dependence on concentration for polystyrene sulfonate ( $M_w = 5400$  Da) at 20.2, 10.1, 5.0, 2.5, and 1.0 mg/mL and Aldrich HA at 20.0, 10.3, 5.2, 2.6, and 1.1 mg/mL in low electrolytic conductivity solutions (0.05% surfactant/0.03%  $\text{NaN}_3$ ) [5].

In normal (Brownian) mode flow FFF, submicrometer particles elute before larger particles, whereas in steric (hyperlayer, lift) mode, micrometer-sized particles elute before smaller particles [8]. Because reversal of the elution order for Aldrich HA and PSS ( $M_w = 5400$ ) was observed (Figures 2 and 3), the conclusion is that the predominant particle size became greater than  $1 \mu\text{m}$  between a concentration of 2.6 and  $5.2 \text{ mg}\cdot\text{mL}^{-1}$ . Peak narrowing also occurred as concentration increased indicating that the range of particle sizes in the sample reduced.

If normal flow FFF predominates during the low ionic strength fractionation of HSS at a concentration of  $1 \text{ mg/mL}$ , the hydrodynamic diameter of the HA is calculated Equation (1) to be  $1.7 \text{ nm}$  at the peak maximum (Figure 4), ranging from  $0.5 \text{ nm}$  to  $3.3 \text{ nm}$  for Suwannee River FA and from  $0.7 \text{ nm}$  to  $4.4 \text{ nm}$  for Suwannee River HA. These values correspond with a hydrodynamic diameter of  $1.5 \text{ nm}$  determined by Lead *et al.* [7] for Suwannee River FA at an ionic strength of  $5 \text{ mM NaCl}$ . The diffusion coefficients are reported [3] for  $1 \text{ mg/mL}$  solutions (normal mode) of 21 FAs/HSS—averaging  $3.0 \times 10^{-10} \text{ m}^2\cdot\text{s}^{-1}$ —that were measured in low ionic strength solution (0.05% surfactant/0.03%  $\text{NaN}_3$ ). Lead *et al.* [7] reported diffusion coefficients of  $3.0 \times 10^{-10} \text{ m}^2\cdot\text{s}^{-1}$  and  $2.9 \times 10^{-10} \text{ m}^2\cdot\text{s}^{-1}$  at pH 5.5 and 7.0, respectively, for Suwannee River FA measured by flow FFF at low ionic strength ( $5 \text{ mM}\cdot\text{NaCl}$ ).

However, if steric flow FFF predominates in low ionic strength solution at a concentration of  $20 \text{ mg}\cdot\text{mL}^{-1}$ , the hydrodynamic diameter of the HA is calculated Equation (2) to be  $160 \mu\text{m}$  (Figure 4) at the peak maximum, which is approximately 30% of the width of the channel (*i.e.*,  $508 \mu\text{m}$ ). At  $10.32 \text{ mg}\cdot\text{mL}^{-1}$  the diameter is  $125 \mu\text{m}$ , and  $100 \mu\text{m}$  at  $5.16 \text{ mg}\cdot\text{mL}^{-1}$ .

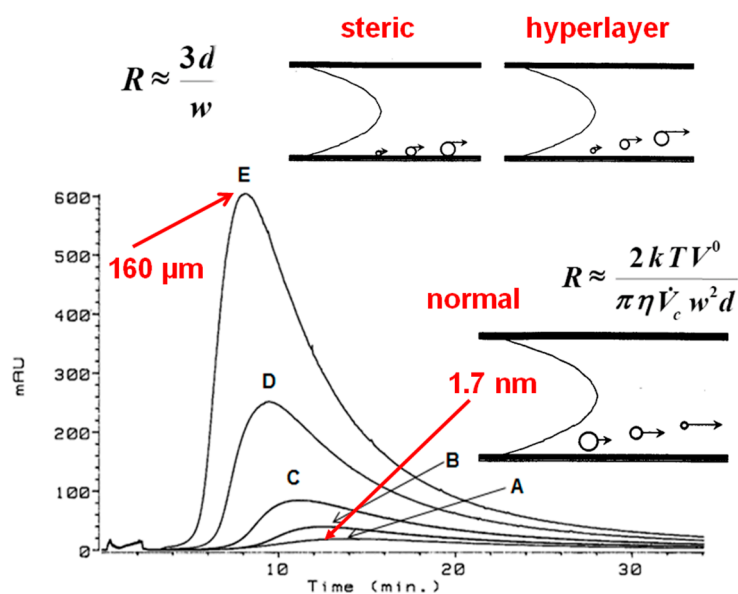


**Figure 4.** Flow FFF fractograms of Aldrich HA in low electrolytic conductivity solutions (0.05% surfactant/0.03%  $\text{NaN}_3$ ) for A—1.1, B—2.6, C—5.2, D—10.3, and E—20.0 mg/mL detected by  $\text{UV}_{254}$ . The hydrodynamic diameters at peak maxima were calculated to be 1.7 nm for A—1.1 mg/L and 160  $\mu\text{m}$  for E—20.0 mg/mL.

The inversion point observed (reversal of retention order between Aldrich HA and PSS ( $M_w = 5400$  Da) at approximately 5 mg/mL (5  $\text{g}\cdot\text{L}^{-1}$ ) of Aldrich HA by flow FFF at low ionic strength corresponds with its reported critical micelle concentration determined by other methods: 7.4  $\text{g}\cdot\text{L}^{-1}$  [9], and that of other HAs as 4  $\text{mg}\cdot\text{mL}^{-1}$  (4  $\text{g}\cdot\text{L}^{-1}$ ) [10], 0.5%–0.6% (5–6  $\text{g}\cdot\text{L}^{-1}$ ) [11], and 8  $\text{g}\cdot\text{dm}^{-3}$  (8  $\text{g}\cdot\text{L}^{-1}$ ) [12].

### 3.1.2. High Electrolytic Conductivity Solutions

In high ionic strength solution, the flow FFF of three types of humic substances exhibited concentration independence (Figure 1b) at 1–10 mg/L concentrations in 0.1 M potassium phosphate (pH 8.1) [4]. The hydrodynamic diameter, calculated using Equation (1), averaged 2.2 nm at the peak maximum and ranged, on average, from 0.84 nm to 6.9 nm (Table 1). Comparably, Lead *et al.* [7] measured the hydrodynamic diameter of Suwannee River FA to be 2.1 nm at 50 mM, and Assemi *et al.* [13] reported hydrodynamic diameters of HSs ranging from 0.99 nm to 3.69 nm as measured by flow FFF in mobile phase ionic strength of 0.08 M.

The diffusion coefficients calculated at the peak maximum for ultraviolet (UV) and fluorescence (FL) detection of three types of HSs at 1–10 mg/L concentrations in high ionic strength solution—0.1 M potassium phosphate (pH 8.1)—averaged  $2.0 \times 10^{-10} \text{ m}^2\cdot\text{s}^{-1}$  (Table 2). The data are comparable to the diffusion coefficients obtained using flow FFF by Lead *et al.* [7] for 10–5000 mg/L Suwannee River fulvic acid (SRFA) which were  $1.9 \times 10^{-10}$  and  $2.2 \times 10^{-10} \text{ m}^2\cdot\text{s}^{-1}$  at pH 5.5 and 7.0 in 50 mM NaCl, respectively.

**Table 1.** Calculation of hydrodynamic diameters at the lower range of the peak ( $d_{\min}$ ), at the upper range of the peak ( $d_{\max}$ ), and at the peak maximum ( $d_p$ ) measured in high electrolytic conductivity solution by ultraviolet (UV) or fluorescence (FL) detection. SRFA: Suwannee River fulvic acid.

| Humic substance               | $d_{\min}$ (nm) | $d_p$ (nm) | $d_{\max}$ (nm) |
|-------------------------------|-----------------|------------|-----------------|
| <b>Ultraviolet detection</b>  |                 |            |                 |
| Aldrich                       | 0.76            | 2.2        | 7.3             |
| Aldrich extract               | 0.73            | 2.3        | 7.8             |
| SRFA                          | 0.83            | 2.0        | 6.0             |
| <b>Fluorescence detection</b> |                 |            |                 |
| Aldrich                       | 0.88            | 2.2        | 7.6             |
| Aldrich extract               | 0.88            | 2.3        | 7.0             |
| SRFA                          | 0.93            | 2.1        | 5.8             |

**Table 2.** Calculation of diffusion coefficients at the peak maximum ( $D_p$ ) measured in high electrolytic conductivity solution by ultraviolet (UV) or fluorescence (FL) detection.

| Humic substance               | $D_p$ ( $\text{m}^2 \text{s}^{-1} \times 10^{10}$ ) |
|-------------------------------|---|
| <b>Ultraviolet detection</b>  |   |
| Aldrich                       | 2.0   |
| Aldrich extract               | 1.9   |
| SRFA                          | 2.2   |
| <b>Fluorescence detection</b> |   |
| Aldrich                       | 1.9   |
| Aldrich extract               | 1.9   |
| SRFA                          | 2.1   |

### 3.2. Dynamic Light Scattering (DLS) of Humic Substances (HSs)

#### 3.2.1. Low Electrolytic Conductivity Solutions

Recently, using DLS, Esfahani *et al.* [2] demonstrated the abiotic reversible self-assembly of FA and HA aggregates in low electrolytic conductivity solutions, providing independent evidence for the existence of HSs aggregates. Particle size distributions in three ranges, *i.e.*, 10–100 nm, 100–1000 nm, and  $>1 \mu\text{m}$  were observed in low electrolytic conductivity solutions with or without added sodium azide (0.03%). Sample concentrations ranged from  $2 \text{ mg}\cdot\text{L}^{-1}$  to  $330 \text{ mg}\cdot\text{L}^{-1}$  expressed as DOC. No particles were observed that were smaller than 10 nm. Although the submicrometer size distributions varied with time, they were always present in all samples analyzed, in contrast to a 5- $\mu\text{m}$ -sized particle that formed within minutes, dissipated, and spontaneously re-formed over turbulent/quiescent cycles. The supramicrometer-sized aggregate self-assembled to a size ten-times greater than the nominal filter size (0.45  $\mu\text{m}$ ). The submicrometer aggregates are postulated to be precursors for the formation of the supramicrometer-sized aggregate. The supramicrometer particle was few-in-number because they were present in intensity- and volume-based DLS spectra but absent in number-based spectra. Because the volume-based particle size distributions are expressed as a percentage, DLS spectra collected at a specific time do not directly show the effects of changing concentration. However, volume-based spectra

graphed over time indicate the increased stability of the supramicrometer-sized aggregate, and the diminished time at which formation of this aggregate was first observed, after onset of quiescence, as concentration increased. Larger or smaller aggregates may exist in these solutions, but were beyond the analytical range of the instrument, *i.e.*, 0.6 nm–6  $\mu$ m.

### 3.2.2. High Electrolytic Conductivity Solutions

The Verdugo research group [14–16] examined seawater (high electrolytic conductivity) amended with sodium azide by DLS and observed only freely dissolved HS polymers (~5–50 nm) during the first 2 h following filtration. Between 5 h and 10 h, nanogels (~100–200 nm) appeared that began to anneal to form larger nanogels. After 60 h, microgels (~3–6  $\mu$ m) formed that were composed of nanogels annealed together. They also demonstrated reversible self-assembly of the microgel after filtration and verified their data using atomic force microscopy, flow cytometry, and environmental scanning electron microscopy. The same general types of particle size distributions, *i.e.*, 10–100 nm, 100–1000 nm, and >1  $\mu$ m, were observed using DLS by Esfahani *et al.* [2], although at low conductivity the microgels formed within minutes as opposed to within hours for the samples examined by the Verdugo research group at high conductivity [14–16]. Significantly, in the DLS research, it should be recognized that the  $\mu$ m-sized-particle formed at the maximum operational range of the instrumentation—the existence of particles larger than 6  $\mu$ m cannot be discounted.

### 3.3. Integrating the Data

The disaggregation/aggregation of HSs (Equation (4)) is here proposed to be a dynamic equilibrium process for which the rate of aggregate formation (at least for some types of aggregates) is controlled by the electrolytic conductivity of the solution:



In low electrolytic conductivity solutions,  $k_1$  and  $k_2$  are larger (the disaggregation/aggregation of HSs occurs more rapidly—in minutes), whereas in high electrolytic conductivity solutions,  $k_1$  and  $k_2$  are smaller (the disaggregation/aggregation of HSs occurs more slowly—in hours). Both the forward and reverse processes appear to be kinetically favored in low electrolytic conductivity solutions. This explains why the fractograms of HSs are broad in low electrolytic conductivity solutions and are more narrow and Gaussian-shaped in high electrolytic conductivity solutions (Figure 1). In flow FFF conducted at high electrolytic conductivity, the time scale of the experiment is too short to allow for the formation of aggregates—therefore, the fractograms are concentration independent.

A substantial degree of variation in the hydrodynamic diameters of HSs has been reported in the data discussed here, overall representing four size ranges with one exception, *i.e.*, (1) <10 nm; (2) 10 nm–6  $\mu$ m; (3) 6–100  $\mu$ m (no representatives in this data for this range); and (4) >100  $\mu$ m. Wershaw and Hayes [17] noted that HAs form micelle-like aggregates above a critical concentration, but DOC molecules form pre-micellar aggregations at natural concentrations. NOM was considered to be a continuum of hydrodynamic diameters by Beckett and Ranville [18]. Tarasevich *et al.* [12] reported that, at low concentrations, HAs exist as individual molecules; as the concentration is increased, they

associate to form supramolecular structures at  $5 \text{ mg} \cdot \text{dm}^{-3}$  ( $5 \text{ mg} \cdot \text{L}^{-1}$ ) and micelles at  $8 \text{ g} \cdot \text{dm}^{-3}$  ( $8 \text{ g} \cdot \text{L}^{-1}$ ). Representative components of the different size ranges probably all dynamically coexist in solution.

### 3.3.1. Aggregates $>100 \mu\text{m}$

Particle sizes greater than  $100 \mu\text{m}$  dominated the flow FFF fractograms at concentrations of approximately  $5 \text{ g} \cdot \text{L}^{-1}$  or greater in low conductivity solutions. Although it can be argued that these concentrations are not environmentally relevant in natural systems, some situations, such as in soils or in wastewaters (and definitely in laboratories), might approach such concentrations. The existence of these aggregates lends support to the micelle/vesicle conceptualization proposed by Wershaw [19].

Manning *et al.* [20] used laser diffraction to measure the particle size distribution by volume of a 10 ppm HA solution and reported particle diameters ranging from  $100 \mu\text{m}$  to greater than  $2500 \mu\text{m}$ , pointing out that a single  $1000 \mu\text{m}$  particle occupies the same volume of HA as 4.6 billion particles that are  $0.6 \mu\text{m}$  in size. Aggregates of this size/type were noted to form in low electrolytic conductivity solution above a specific concentration (Figure 1a); however, the data presented here do not establish whether or not aggregates of this size/type form in high electrolytic conductivity solutions.

Contrary to some comments in the literature, the critical micelle concentration is not the concentration at which micelles first begin to form. Speaking generally about micelles (not specifically HS micelles), Mukerjee and Mysels [21] stated that, depending on the sensitivity of the analysis, micelles may be undetectable in dilute solutions of the constituent monomers, and at low concentrations, the additional solute molecules which form micelles may be very low until a concentration is reached at which nearly all additional solute molecules form micelles. That concentration is recognized as the critical micelle concentration. Therefore, micelles may exist in solutions less concentrated than the critical micelle concentration, but be undetectable.

### 3.3.2. Aggregates $6\text{--}100 \mu\text{m}$

Significantly, in the DLS research reported here, the maximum operational range of the instrumentation was  $6 \mu\text{m}$ . In the steric mode flow FFF experiments at low electrolytic conductivity, the smallest particle measured was  $100 \mu\text{m}$ . Therefore, in this data set, no aggregates were detected in this size category; however, the existence of such particles cannot be discounted.

### 3.3.3. Aggregates $10\text{--}100 \text{ nm}$ , $100\text{--}1000 \text{ nm}$ , and $1\text{--}6 \mu\text{m}$

Are aggregates in these size ranges densely packed associations of HS molecules, or are they primarily water-based hydrogels? Also, if they exist as weakly associated hydrogel structures, how will shear forces in FFF affect these types of aggregates?

By DLS, the formation of aggregates in each of these three size ranges was observed to occur in minutes in HS solutions of low ionic strength [2], but required hours to days to form in HS solutions of seawater at high ionic strength [14–16]. The presence of an excess amount of counterions (high conductivity) could be hypothesized to neutralize the negatively charged HSs and promote hydrophobic association, but that is counterintuitive to the concept of the slow formation of the aggregates at high ionic strength. However, if the aggregates in the  $10\text{--}100 \text{ nm}$ ,  $100\text{--}1000 \text{ nm}$ , and  $1\text{--}6 \mu\text{m}$  particle size distributions are truly hydrogels (nanogels and microgels [14–16]), then the hydrophilic charged form

of HSs would be more water-friendly, and would explain why they form more readily at low ionic strength. Chin *et al.* [16] described the DOC hydrogels as an ionic-bond-stabilized tangled network, rather than a covalently crosslinked network. The self-assembled marine microgel in seawater was envisioned to be composed of approximately 1% solids, which represents a higher local concentration of organic matter in the particle than in the surrounding water environment [16]. If the concentration of organic matter in the hydrogel is as low as 1%, it may not be possible to identify these aggregates in flow FFF with ultraviolet or fluorescence detection.

The 1–6  $\mu\text{m}$ -sized-particle was observed to reversibly self-assemble at very low DOC concentrations ( $\leq 2$  ppm) in simulated and environmental water samples [2,16]. This supramicrometer-sized particle was determined to be few-in-number because they were present in intensity- and volume-based DLS spectra but absent in number-based spectra [2]. Manning *et al.* [20] used two instruments with a combined operational size range from  $<100$  nm to  $2000 \mu\text{m}$  to evaluate the effect of chemical matrix and measured the size of aggregates of Aldrich humic acid solutions ranging in ionic strength. Their light scattering research of humic acid also led to the conclusion that most of the volume existed in a few particles of large diameter. At pH 10 and 10 ppm (Day 4), they established that most particle diameters were in the 0.5 to 0.6  $\mu\text{m}$  range, over 90% were smaller than 0.8  $\mu\text{m}$ , and 99.9% were smaller than 1  $\mu\text{m}$ .

Turbulence, in the form of pouring, filtering, or shaking, was demonstrated by DLS [2] to have a disruptive effect on the  $>1 \mu\text{m}$ -sized particle (microgel), after which it reversibly self-assembled upon re-establishment of quiescence. Conversely, by DLS, the presence of particles in the 10 nm to 1  $\mu\text{m}$ -size range (nanogels) was observed before, and immediately after, inducing turbulence. The Verdugo group [14–16], posits that the microgels were formed by annealing of the nanogels, which could explain the different character observed in response to turbulence for these two entities. Therefore, the turbulence generated by shear forces of the cross and channel flows in flow FFF can be postulated to be more disruptive to particles in the 1–6  $\mu\text{m}$  range. The application of flow FFF to the analysis of hydrogels of humic and other materials is an exciting research front to be pursued.

#### 3.3.4. Aggregates $<10$ nm

Aggregates smaller than 10 nm were not observed in either of the DLS studies reviewed here. Verdugo [14] illustrated the presence of extended free DOC polymers in angstrom-sized molecular dimensions by atomic force microscopy and environmental scanning electron microscopy. Conversely, aggregates in this size range were measured by flow FFF at both low and high ionic strength mobile phases.

The smallest unit size reported here is 0.5 nm or 5 Angstroms, which approaches the size expected for individual molecules. The largest size in this range determined by flow FFF, *i.e.*, 7.8 nm, can be considered to consist of several humic subunits joined together in extended or linear random-coiled chains—and most nearly deserve to be called macromolecules of all the aggregates studied—different in character compared to the members of the larger aggregate size ranges.

#### 4. Conclusions

FAs and HAs are fascinating chemicals. The more they are studied, the greater is our respect for their complexity. The question that began as—*Why is the flow field-flow fractionation of fulvic and humic acids concentration independent at high ionic strength and concentration dependent at low ionic strength?*—led to investigation of the fundamental differences in the character of HS aggregates as ionic strength varies. The data presented here are interpreted to indicate that the kinetics of the association-dissociation equilibrium for HSs favor the increased rate of aggregation in low ionic strength solutions in preference to high ionic strength solutions. In flow FFF conducted at high electrolytic conductivity, the time scale of generating the fractogram is too short to allow for the formation of aggregates >10 nm—therefore, the fractograms are concentration independent and Gaussian. In flow FFF conducted at low electrolytic conductivity, the disaggregation/aggregation processes are fast enough to be observed within the time scale of generating the fractogram—therefore, the fractograms are concentration dependent and non-Gaussian.

Eventually, equilibrium will be reached in both low and high ionic strength solutions; however, the equilibrium state itself does not reveal anything about how kinetically fast it will be reached. The kinetics of the disaggregation/aggregation equilibrium best supports conceptualization that the HS aggregates between 10 nm and 6  $\mu\text{m}$  are hydrogels rather than densely packed associations of HS molecules. If the 1–6  $\mu\text{m}$  particle size distribution is truly a hydrogel, and if the >100  $\mu\text{m}$  particle is truly a micelle or vesicle (resulting from hydrophobic association) they will have different properties that can be examined by further research. To build upon this research, future examination of the fractionation of FAs and HAs as ionic strength varies should be pursued by coupling FFF with light scattering detectors and with more sophisticated inductively coupled plasma-mass spectrometry (ICP-MS) or ICP-atomic emission spectroscopy (AES) detectors to investigate the influence of different counterions on the formation of aggregates.

#### Conflicts of Interest

The author declares no conflict of interest.

#### References

1. Zularisam, A.; Ismail, A.F.; Salim, M.; Sakinah, M.; Ozaki, H. The effects of natural organic matter (NOM) fractions on fouling characteristics and flux recovery of ultrafiltration membranes. *Desalination* **2007**, *212*, 191–208.
2. Esfahani, M.R.; Stretz, H.A.; Wells, M.J.M. Abiotic reversible self-assembly of fulvic and humic acid aggregates in low electrolytic conductivity solutions by dynamic light scattering and zeta potential investigation. *Sci. Total Environ.* **2015**, *537*, 81–92.
3. Dycus, P.J.M.; Healy, K.D.; Stearman, G.K.; Wells, M.J.M. Diffusion coefficients and molecular weight distributions of humic and fulvic acids determined by flow field-flow fractionation. *Sep. Sci. Technol.* **1995**, *30*, 1435–1453.

4. Schmit, K.H.; Wells, M.J.M. Preferential adsorption of fluorescing fulvic and humic acid components on activated carbon using flow field-flow fractionation analysis. *J. Environ. Monit.* **2002**, *4*, 75–84.
5. Dycus, P.J.M. Macromolecules: Separation by Flow Field-Flow Fractionation. Master's Thesis, Tennessee Technological University, Cookeville, TN, USA, 1993.
6. Benincasa, M.A.; Cartoni, G.; Imperia, N. Effects of ionic strength and electrolyte composition on the aggregation of fractionated humic substances studied by flow field-flow fractionation. *J. Sep. Sci.* **2002**, *25*, 405–415.
7. Lead, J.R.; Wilkinson, K.J.; Balnois, E.; Cutak, B.J.; Larive, C.K.; Assemi, S.; Beckett, R. Diffusion coefficients and polydispersities of the Suwannee River fulvic acid: Comparison of fluorescence correlation spectroscopy, pulsed-field gradient nuclear magnetic resonance, and flow field-flow fractionation. *Environ. Sci. Technol.* **2000**, *34*, 3508–3513.
8. Martin, M.; Beckett, R. Size Selectivity in field-flow fractionation: Lift mode of retention with near-wall lift force. *J. Phys. Chem. A* **2012**, *116*, 6540–6551.
9. Guetzloff, T.F.; Rice, J.A. Does humic acid form a micelle? *Sci. Total Environ.* **1994**, *152*, 31–35.
10. Smejkalova, D.; Piccolo, A. Aggregation and disaggregation of humic supramolecular assemblies by NMR diffusion ordered spectroscopy (DOSY-NMR). *Environ. Sci. Technol.* **2007**, *42*, 699–706.
11. Lei, W.; Zhu, Z.; Wang, Z.; Chen, P. Surface activity of humic acids. *Ranliao Huaxue Xuebao* **1986**, *14*, 177–181. (In Chinese)
12. Tarasevich, Y.I.; Dolenko, S.A.; Trifonova, M.Y.; Alekseenko, E.Y. Association and colloid-chemical properties of humic acids in aqueous solutions. *Colloid J.* **2013**, *75*, 207–213.
13. Assemi, S.; Newcombe, G.; Hepplewhite, C. Beckett, R. Characterization of natural organic matter fractions separated by ultrafiltration using flow field-flow fractionation. *Water Res.* **2004**, *38*, 1467–1476.
14. Verdugo, P. Marine microgels. *Annu. Rev. Mar. Sci.* **2012**, *4*, 375–400.
15. Verdugo, P.; Santschi, P.H. Polymer dynamics of DOC networks and gel formation in seawater. *Deep Sea Res. Part II Top. Stud. Oceanogr.* **2010**, *57*, 1486–1493.
16. Chin, W.-C.; Orellana, M.V.; Verdugo, P. Spontaneous assembly of marine dissolved organic matter into polymer gels. *Nature* **1998**, *391*, 568–572.
17. Wershaw, R.L.; Hayes, T.M. Solubilization of Anthropogenic Compounds by Humic Substances. In *Humic Substances and Chemical Contaminants*; Clapp, C.E., Hayes, M.H.B., Senesi, N., Bloom, P.R., Jardine, P.M., Eds.; Soil Science Society of America: Madison, WI, USA, 2001; pp. 165–176.
18. Beckett, R.; Ranville, J. Natural Organic Matter. In *Interface Science in Drinking Water Treatment*; Newcombe, G., Dixon, D., Eds.; Elsevier: London, UK, 2006; pp. 299–315.
19. Wershaw, R.L. *Membrane-Micelle Model for Humus in Soils and Sediments and its Relation to Humification*; Technical Report for US Geological Survey; U.S. Geological Survey (USGS): Denver, CO, USA, 1994.
20. Manning, T.J.; Sherrill, M.L.; Bennett, T.; Land, M.; Noble, L. Effect of chemical matrix on humic acid aggregates. *Fla. Sci.* **2004**, *67*, 266–280.

21. Mukerjee, P.; Mysels, K.J. *Critical Micelle Concentrations of Aqueous Surfactant Systems*; National Bureau of Standards: Washington, D.C., USA, 1971; p. 4.

© 2015 by the author; licensee MDPI, Basel, Switzerland. This article is an open access article distributed under the terms and conditions of the Creative Commons Attribution license (<http://creativecommons.org/licenses/by/4.0/>).